© 2015. Published by The Company of Biologists Ltd | Development (2015) 142, 99-107 doi:10.1242/dev.111161

RESEARCH ARTICLE

Vangl2 cooperates with Rab11 and Myosin V to regulate apical constriction during vertebrate gastrulation

Olga Ossipova, Ilya Chuykin, Chih-Wen Chu and Sergei Y. Sokol*

ABSTRACT

Core planar cell polarity (PCP) proteins are well known to regulate polarity in *Drosophila* and vertebrate epithelia; however, their functions in vertebrate morphogenesis remain poorly understood. In this study, we describe a role for PCP signaling in the process of apical constriction during *Xenopus* gastrulation. The core PCP protein Vangl2 is detected at the apical surfaces of cells at the blastopore lip, and it functions during blastopore formation and closure. Further experiments show that Vangl2, as well as Daam1 and Rho-associated kinase (Rock), regulate apical constriction of bottle cells at the blastopore and ectopic constriction of ectoderm cells triggered by the actin-binding protein Shroom3. At the blastopore lip, Vangl2 is required for the apical accumulation of the recycling endosome marker Rab11. We also show that Rab11 and the associated motor protein Myosin V play essential roles in both endogenous and ectopic apical constriction, and might be involved in Vangl2 trafficking to the cell surface. Overexpression of Rab11 RNA was sufficient to partly restore normal blastopore formation in Vangl2-deficient embryos. These observations suggest that Vangl2 affects Rab11 to regulate apical constriction during blastopore formation.

KEY WORDS: Planar cell polarity, Vangl2, Blastopore, *Xenopus*, Rab11, Myosin V, Daam1, Rho-associated protein kinase

INTRODUCTION

The planar cell polarity (PCP) pathway was discovered as a molecular pathway that regulates the polarization of epithelial tissues in *Drosophila* embryos (Axelrod, 2009; Gubb and Garcia-Bellido, 1982; Vinson and Adler, 1987; Wang and Nathans, 2007). Cell polarization in the plane of the epithelial tissue is established by the core PCP components Frizzled, Disheveled, Van Gogh/Stbm, Prickle and Flamingo, which form separate protein complexes distributed to the opposite sides of each cell. This non-homogeneous distribution in the epithelial tissue is reinforced through positive-feedback regulation (Tree et al., 2002a). Although the roles and molecular interactions of PCP proteins in fly epithelia have been studied in some detail (Bastock et al., 2003; Jenny et al., 2005; Tree et al., 2002b; Wu and Mlodzik, 2008), accumulating evidence indicates that vertebrate PCP components have functions that are not directly related to cell polarity in the plane of the tissue. Vertebrate PCP proteins are now known to control a large number of developmental processes, including inner ear polarity (Montcouquiol et al., 2003), left-right patterning (Antic et al., 2010; Borovina et al., 2010; Hashimoto et al., 2010; Song et al., 2010), mesodermal convergent extension (Keller, 2002; Sokol, 2000), neural tube closure (Copp and Greene, 2010; Sokol, 1996), neurite extension, neuronal migration, branching morphogenesis and vascular development (Carroll and Yu, 2012; Gray et al., 2011; Jessen et al., 2002; Ju et al., 2010; Tissir and Goffinet, 2013; Yates et al., 2010b). The molecular mechanisms underlying this pleiotropic behavior of PCP proteins in morphogenesis remain poorly understood.

Xenopus gastrulation is one of the extensively studied vertebrate models of early morphogenesis, which involves multiple cell behaviors. Gastrulation starts with the formation of the dorsal blastopore lip, characterized by the appearance of bottle-shaped cells. The bottle cells undergo apical constriction, a universal process, during which cells elongate while reducing their apical surface (Sawyer et al., 2010). At the same time, head mesoderm cells migrate towards the future anterior of the embryo. Dorsal lip converts into a 'smile', which subsequently spreads around the blastopore. This coordinated apical constriction promotes mesendoderm involution, which results in the entire embryo surface being covered by ectoderm. The circumference of the blastopore gradually narrows, and the blastopore is closed at the end of gastrulation, while dorsal axial and paraxial mesoderm cells undergo mediolateral interactions, known as dorsal convergent extension (Keller, 2002). Although many studies address the roles of PCP proteins in convergent extension (Gray et al., 2011; Habas et al., 2001; Sokol, 2000; Wallingford, 2012), there is sparse evidence for the function of PCP proteins in other cell behaviors during gastrulation.

The analysis of PCP signaling in vertebrate early development has been limited by insufficient knowledge of the localization of endogenous proteins at the onset of gastrulation. Therefore, we initiated an analysis of the localization and function of endogenous PCP components in morphogenetic processes that precede convergent extension in *Xenopus* embryos. Here, we describe an apical enrichment of Vangl2 at the blastopore lip during gastrulation and document the functional roles of Vangl2 and the downstream Wnt/PCP components Daam1 and Rock in the apical constriction of bottle cells. In embryos from which Vangl2 has been depleted, Rab11 recycling endosomes mislocalize from the apical junctions to the cytoplasm. Furthermore, we find that Rab11 vesicles function together with Myosin V to regulate apical constriction of blastopore cells. Our findings suggest that PCP signaling regulates apical constriction, at least in part, by directing Rab11-dependent trafficking to the apical surface.

RESULTS

Apical accumulation of Vangl2 at the blastopore lip

Staining of gastrula-stage embryo sections with anti-Vangl2 antibodies revealed an accumulation of immunoreactivity at the apical surface near the blastopore lip, although some signal was also detected at the basolateral cell cortex (Fig. 1A). The enrichment of Vangl2 at the apical surface was similar to the accumulation of apical pigment granules (Fig. 1B) and phosphorylated Myosin II

Department of Developmental and Regenerative Biology, Icahn School of Medicine at Mount Sinai, New York, NY 10029, USA.

*Author for correspondence (sergei.sokol@mssm.edu)

Received 9 April 2014; Accepted 27 October 2014

Development (2015) 142, 99-107 doi:10.1242/dev.111161

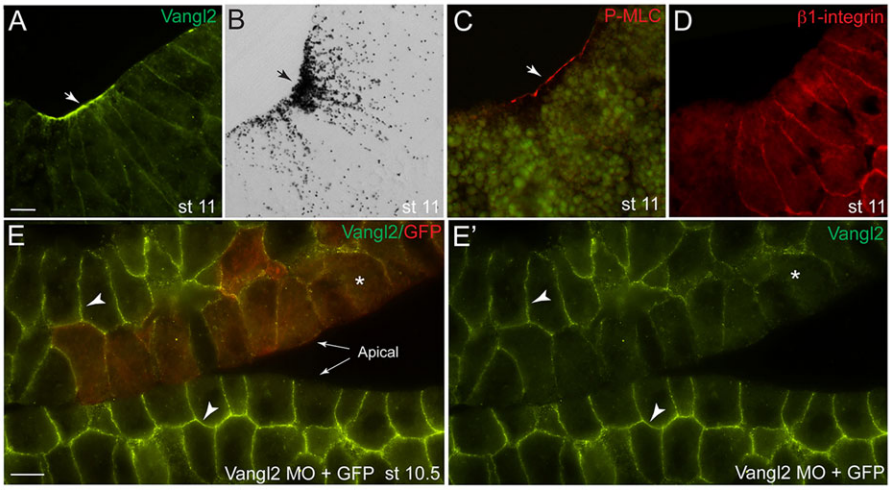

Fig. 1. Subcellular distribution of Vangl2 at the blastopore lip. (A-D) Parasagittal sections of stage (st) 11 embryos showing the blastopore area (arrows). (A) Immunohistochemical staining demonstrating apical and basolateral localization of endogenous Vangl2. (B) Bright-field view of a similar embryo section shows extensive pigmentation in the constricting blastopore cells. (C) Staining with antibodies against pMLC. (D) Basolateral localization of β1-integrin in bottle cells. (E,E′) Subcellular distribution of Vangl2 in the superficial and the inner ectoderm cells. (E) Mosaic distribution of Vangl2 MO with GFP RNA as a lineage tracer (red) confirms Vangl2 antibody specificity. (E′) Green channel only. Arrowheads point to Vangl2 staining in E,E′; asterisks indicate lack of staining. Two embryo sections are shown side-by-side to illustrate Vangl2 depletion. Scale bars: 20 µm.

regulatory light chain (pMLC, Fig. 1C), which mark bottle cells undergoing apical constriction at the beginning of gastrulation (Choi and Sokol, 2009; Lee and Harland, 2007). By contrast, staining for β1-integrin showed that this protein remained basolateral in both superficial ectoderm and constricting bottle cells (Fig. 1D; supplementary material Fig. S1A,B), indicating that the observed changes are specific to Vangl2.

In embryonic ectoderm, Vangl2 was distributed to the basolateral domain of superficial cells and was enriched at the outermost ends of inner cells (Fig. 1E; supplementary material Fig. S1A). To confirm staining specificity, we generated mosaic embryos, in which some cells were depleted of Vangl2 by the use of a previously characterized antisense morpholino oligonucleotide (MO) (Darken et al., 2002). The immunostaining for Vangl2 decreased substantially in these cells, confirming that the antibody is specific to Vangl2 (Fig. 1E,E′). On western blots, this antibody detected GFP- and HA-tagged Vangl2 in gastrula-stage embryo lysates and revealed a specific 60 kDa protein band, which corresponds to endogenous Vangl2 (supplementary material Fig. S1C).

The apical distribution of Vangl2 was not detected before the onset of gastrulation, at stages 9.5 and 10− (supplementary material Fig. S1D,E; data not shown). At stage 10+, the apical localization of Vangl2 was restricted to the dorsal blastopore lip, but it became circumferential at later stages, correlating with the formation of bottle cells at the blastopore ring (supplementary material Fig. S1F,G). These results indicate that Vangl2 is basolaterally localized in superficial blastula cells, but becomes apically accumulated in blastopore bottle cells.

Vangl2 is essential for both endogenous and ectopic apical constriction during gastrulation

Given the localization of Vangl2 in apically constricting cells during gastrulation, we examined the role of Vangl2 in blastopore formation and tissue involution. Interference with Vangl2 function using Vangl2 MO resulted in the inhibition of blastopore formation at the onset of gastrulation in ∼80% of injected embryos (n=99, Fig. 2A,B). A knockdown of Daam1, another component of Wnt/PCP signaling (Habas et al., 2001), similarly resulted in the suppression of bottle cell formation (58%, n=50, Fig. 2C). By contrast, control MO or GFP RNA did not have significant effects on blastopore formation (Fig. 2A,D). Corresponding to these morphological changes, staining for pMLC and F-actin was suppressed in Vangl2 morphants (Fig. 2E,F; supplementary material Fig. S2F,G). Bottle cells were also locally inhibited at later stages in embryos injected with Vangl2 MO into either dorsal or ventrolateral blastomeres at the 8-16 cell stage (supplementary material Fig. S2A-E). Because the overexpression of Vangl2 did not alter the expression of mesodermal and endodermal fate markers (Darken et al., 2002), our results suggest that Vangl2 is involved in the apical constriction of bottle cells during gastrulation, rather than playing a role in cell specification, as reported in different contexts (Cortijo et al., 2012; Lake and Sokol, 2009).

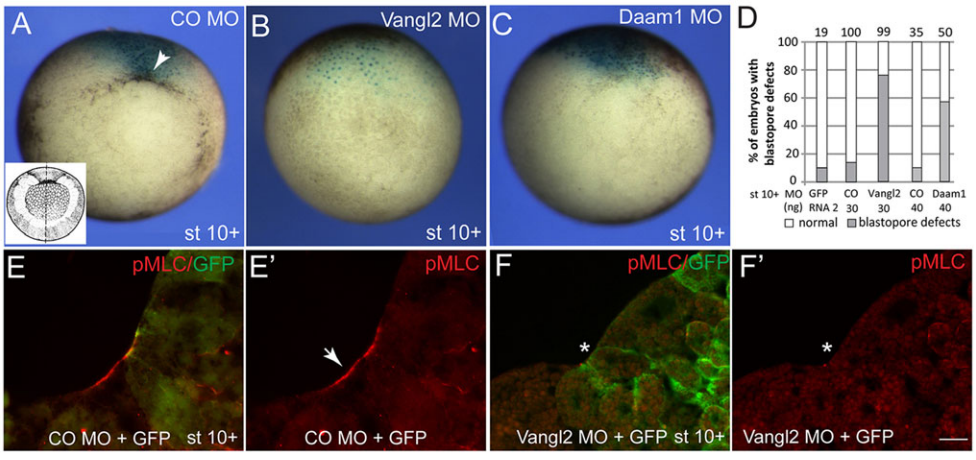

Fig. 2. Vangl2 and Daam1 are required for blastopore formation. (A-D) Blastopore defects in embryos depleted of Vangl2 and Daam1. Embryos were injected with control (CO) MO, Vangl2 MO or Daam1 MO, as indicated, and *lacZ* RNA (150 pg) as a lineage tracer. The vegetal view is shown. Dorsal is to the top. A schematic of a gastrula embryo is shown in the inset in A. (A-C) Blastopore formation (arrowhead) is inhibited in stage (st) 10+ embryos by Vangl2 MO or Daam1 MO. (D) Quantification of the effect. (E,E′) Myosin II light chain (MLC) phosphorylation at the blastopore lip (arrow) in control embryos. (F,F′) Vangl2 MO inhibits Myosin II activation (asterisk) in apically constricting cells. Scale bar: 20 µm.

Development (2015) 142, 99-107 doi:10.1242/dev.111161

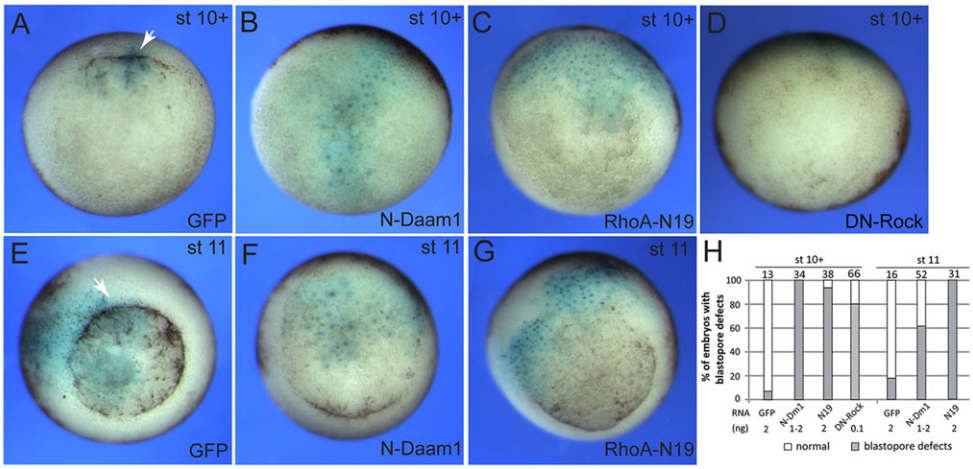

Fig. 3. Roles of downstream PCP components in bottle cell formation. (A-D) Early blastopore defects in embryos expressing dominant interfering constructs for PCP and Rock pathway components. Embryos were injected with GFP, N-Daam1 or RhoA-N19 RNAs (2 ng each) or DN-Rock RNA (0.1 ng), together with *lacZ* RNA (0.15 ng) as lineage tracer. Vegetal view of stage (st) 10+ embryos is shown. Dorsal is to the top. (E-G) Embryos expressing N-Daam1 and RhoA-N19 display delayed blastopore closure at stage 11. Arrows in A and E indicate blastopore lip in control GFP-expressing embryos. (H) Quantification of the effect. N-Dm1, N-Daam1; N19, RhoA-N19.

To extend our observations regarding the role of Vangl2 at the onset of gastrulation, we further examined whether additional PCP components, such as Daam1 and Rock (Habas et al., 2001; Marlow et al., 2002; Winter et al., 2001), are involved in blastopore formation. Using the known dominant interfering constructs, we established a requirement for both Daam1 and Rock in apical constriction, both at the beginning and during the course of gastrulation (Fig. 3). These findings support the view that the Wnt/PCP pathway is involved in this morphogenetic process.

Bottle cells originate as a subpopulation of endodermal cells, which are influenced by many embryonic inducing and patterning factors secreted from the organizer and the surrounding tissues (Harland and Gerhart, 1997). To dissociate the fate specification process that occurs in bottle cells from morphogenetic events, we took advantage of an ectopic model, in which embryonic ectoderm undergoes apical constriction in response to overexpression of Shroom3 (here referred to as Shroom for simplicity), an actin-binding PDZ-containing protein (Haigo et al., 2003; Hildebrand and Soriano, 1999) (Fig. 4). As expected, Shroom RNA triggered efficient constriction and the accompanying hyper-pigmentation of animal pole ectoderm at the time corresponding to the beginning of gastrulation. This ectopic apical constriction was substantially inhibited by Vangl2 MO, but not by the control MO (Fig. 4A-D), reinforcing the view that Vangl2 functions in this morphogenetic process. Moreover, the amino-terminal fragment of Daam1 and a dominant interfering construct of zebrafish Prickle1, from which the PET/LIM domains have been deleted (Carreira-Barbosa et al., 2003; Takeuchi et al., 2003), also suppressed Shroom-mediated ectopic apical constriction in embryonic ectoderm (Fig. 4E-H), supporting a general role for Wnt/PCP signaling in the apical constriction of blastopore bottle cells.

Rab11 is apically localized at the blastopore lip in a Vangl2-dependent manner

Previous work has documented a role for endocytosis in apical constriction during gastrulation (Lee and Harland, 2010), and we wanted to assess the possibility that components of vesicular trafficking might function downstream of PCP signaling in apical constriction. We examined the localization of Rab11, a marker of the recycling endosome (Bryant et al., 2010; Mizuno-Yamasaki et al., 2012), which has been implicated in planar polarization of *Xenopus* multiciliated skin cells (Kim et al., 2012) and the neural tube

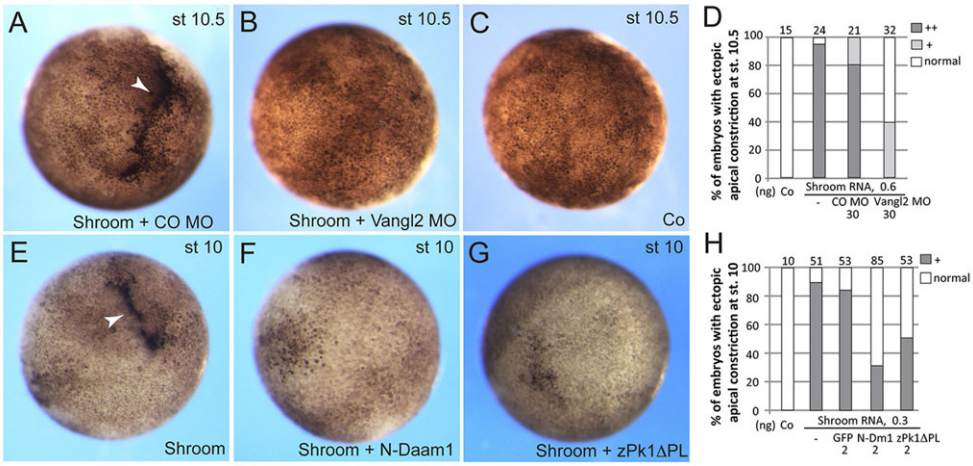

Fig. 4. Interference with the PCP pathway prevents Shroom-induced apical constriction. Early embryos were animally injected with FLAG-Shroom RNA (50 pg) and other RNAs or MOs as indicated. (A-D) Vangl2 depletion inhibits Shroom-dependent ectopic apical constriction (arrowhead). CO, control. (A-C) Representative embryo images at stage (st) 10.5. (D) Quantification of the data, numbers of embryos with strong, mild and no ectopic constriction are presented. Strong (++) apical constriction involves hyperpigmentation and the accompanying tissue invagination, mild (+) constriction is frequently visible as diffuse hyperpigmentation in the absence of tissue indentation. (E-H) Inhibitory effects of N-Daam1 and zPk1ΔPL on Shroom-dependent apical constriction in stage 10 embryos. (H) Quantification of the data. +indicates ectopic apical constriction; 'normal' indicates no constriction.

Development (2015) 142, 99-107 doi:10.1242/dev.111161

(Ossipova et al., 2014). In early ectoderm and in the non-constricting epithelial layer of the marginal zone cells, Rab11 is detected largely at cell junctions (supplementary material Fig. S3A-C) (Ossipova et al., 2014). At late blastula stages, we observed the broad apical accumulation of Rab11 at the marginal zone (supplementary material Fig. S3A-C). Rab11 became strongly enriched near the blastopore lip at the onset of gastrulation (Fig. 5A-C). Co-staining of embryo sections with anti-pMLC antibodies revealed tight colocalization with the bottle cell population (Fig. 5D-D″), indicating that Rab11 might function largely in apically constricting blastopore cells.

We next tested whether Vangl2 might influence the localization of Rab11 at the apical surface of blastopore cells. In Vangl2-depleted embryos, the apical staining for Rab11 became largely undetectable (Fig. 5E,F). Similarly, in superficial ectoderm cells, the localization of Rab11 changed from junctional to cytoplasmic after Vangl2 MO injection (Fig. 5G,H). These findings support the hypothesis that Rab11 is regulated by PCP signaling and could play a role in blastopore formation.

Rab11 and the associated motor protein Myosin V function during blastopore lip formation and apical constriction

Based on our observations, we hypothesize that Vangl2 functions in gastrulation by regulating the localization of Rab11. Therefore, we studied a function for Rab11 in blastopore formation using a dominant-negative mutant, Rab11S25N (Kim et al., 2012). Rab11S25N, but not the wild-type Rab11, interfered with the appearance of the dorsal lip and delayed blastopore closure (Fig. 6A-C,G). This corresponded to the disappearance of pMLC staining from the blastopore lip (Fig. 6D-F). Blastopore formation was also inhibited when Rab11 was depleted with a previously characterized specific MO (Kim et al., 2012), further supporting a role for Rab11 in apically constricted blastopore cells (Fig. 6G). These effects were morphologically similar to the effects of a dominant-negative Dynamin construct, which interferes with clathrin-dependent endocytosis (data not shown). No change was detected in the expression of several molecular markers, including *Chordin*, *Goosecoid*, *FoxD3*, *Xbra* and *Gef3.2* (GenBank accession number: NM_001096674.1), which are characteristic for mesendodermal cells abutting the blastopore (Fig. 6H). These observations indicate that Rab11 acts in morphogenetic processes rather than patterning processes leading to blastopore formation.

Given that Rab11 is required for blastopore formation and that its apical enrichment depends on Vangl2, we hypothesized that Vangl2 controls apical constriction by modulating Rab11 localization and function. We then tested whether Rab11 RNA can rescue Vangl2-deficient embryos. Whereas embryos injected with Vangl2 MO failed to form the dorsal blastopore lip at stage 10/10+, the majority of Vangl2-depleted embryos that were co-injected with either wild-type or constitutively active Q70L Rab11 RNA, but not with GFP RNA, showed normal onset of gastrulation (Fig. 6I; supplementary material Fig. S4). These findings are consistent with the hypothesis that Vangl2, at least in part, controls gastrulation and bottle cell morphology by modulating Rab11-dependent vesicular trafficking.

Besides establishing the requirement for Vangl2 in Rab11 localization, we examined whether Rab11 knockdown would affect Vangl2 subcellular distribution (supplementary material Fig. S5). The membrane-associated Vangl2 staining was consistently reduced in apically constricted bottle cells and in non-constricted ectoderm cells in which Rab11 was depleted. These findings suggest that Vangl2 is delivered to the cell surface by Rab11-mediated endocytic recycling.

We next wanted to confirm the role of Rab11 in the constricting cells using an alternative approach. Because Myosin V is a motor protein that functions together with Rab11 in apical vesicular

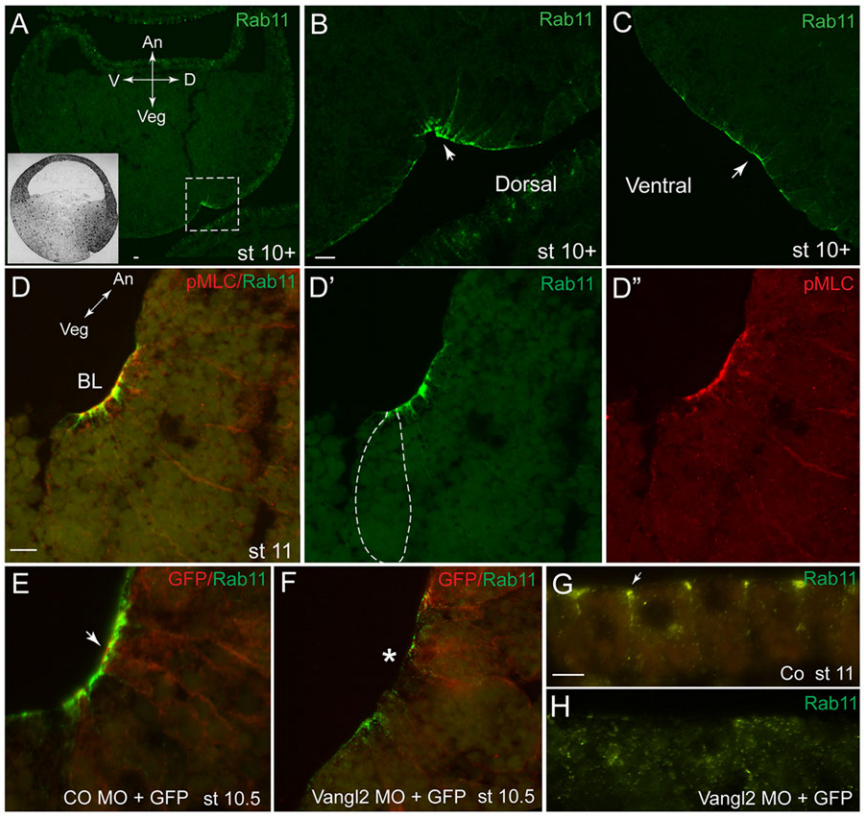

Fig. 5. Rab11 is apically localized at the blastopore lip in a Vangl2-dependent manner. (A-C) Cross-sections of early gastrula embryos [stage (st) 10+] immunostained for Rab11. An, animal; Veg, vegetal; D, dorsal; V, ventral axes are indicated. The dashed box in A corresponds to the magnified image shown in B. The inset in A shows a schematic of a sectioned gastrula-stage embryo. (D-D″) Co-immunostaining of Rab11 and pMLC. In D′, bottle cell morphology is indicated by the dashed line. BL, blastopore lip. (E,F) Rab11 localization at the blastopore requires Vangl2. Rab11 staining at the blastopore area of embryos co-injected with 30 ng of Vangl2 MO and 100 pg of GFP RNA. A cross-section of a stage 10.5 embryo is shown. The arrow in E points to bottle cells; the asterisk in F indicates inhibited apical constriction. CO, control. (G,H) Sections of ectoderm immunostained for Rab11, apical is to the top. (G) Rab11 is at the apical cell junctions (arrow) in control ectoderm. (H) Rab11 is more cytoplasmic in cells depleted of Vangl2. Scale bars: 20 µm in B,G, 10 µm in D.

Development (2015) 142, 99-107 doi:10.1242/dev.111161

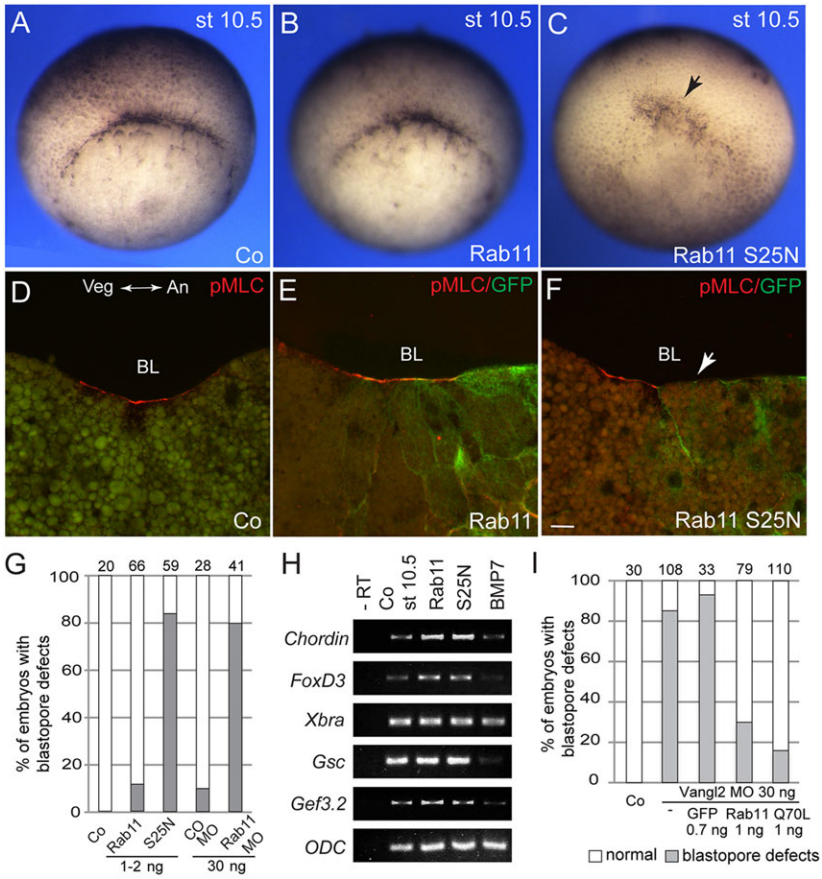

Fig. 6. The involvement of Rab11 in blastopore formation and myosin II activation. (A-F) Embryos were co-injected with RNAs encoding wild-type Rab11 or Rab11S25N and GFP RNA as a lineage tracer. Alternatively, Rab11 was depleted with a specific Rab11 MO. Co, control. (A-C) *En face* view of the injected embryo morphology at stage (st) 10.5. The arrow points to the inhibited blastopore lip. (D-F) Inhibition of pMLC staining in Rab11S25N-expressing embryos. A cross-section is shown with animal pole to the right. The arrow shows lack of the pMLC signal. BL, blastopore lip; Veg, vegetal; An, animal. Scale bar: 20 µm. (G) Quantification of the results. The total number of embryos per group is shown at the top of each column. (H) Mesendodermal marker expression in embryos (stage 10.5) with manipulated Rab11 function. (I) Rab11 rescues blastopore formation in Vangl2-depleted embryos. Both dorsal blastomeres of four-cell embryos were injected with 30 ng of Vangl2 MO and 1 ng of RNA encoding wild-type Rab11, Rab11Q70L or GFP. Data are shown as the frequency of embryos with dorsal lip defects scored at stage 10+.

trafficking (Bryant et al., 2010; Li et al., 2007; Roland et al., 2011), we assessed Myosin V involvement in blastopore formation and apical constriction. We expressed Myosin V tail (MyoVT), a dominant interfering construct lacking the motor domain, which mimics the loss-of-function phenotype in mouse cells (Lapierre et al., 2001; Wu et al., 1998). Blastopore formation and apical accumulation of Rab11 were inhibited at the site of MyoVT RNA injection (Fig. 7A-E). MyoVT aggregates accumulated in the cytoplasm of the injected cells and colocalized with endogenous Rab11, altering its normal apical distribution at the blastopore (Fig. 7D,E). No changes in Rab11 protein distribution were detected in samples injected with control RNA (data not shown). Finally, we observed an inhibitory effect of MyoVT on ectopic apical constriction of embryonic ectoderm in response to Shroom (Fig. 7F,G). Taken together, these experiments support the view that Rab11 cooperates with Myosin V to regulate apical constriction during gastrulation.

DISCUSSION

To extend the known roles of PCP proteins in convergent extension movements during vertebrate gastrulation, this study assessed the localization and function of the core PCP component Vangl2 in the formation of bottle cells during *Xenopus* gastrulation. Using antibodies specific to *Xenopus* Vangl2, we show that Vangl2 is basolaterally localized in superficial ectoderm but appears to become enriched at the apical surface of blastopore cells undergoing apical constriction. This change parallels the apical accumulation of F-actin and pMLC (Lee and Harland, 2007). Although β1-integrin is similarly localized at the basolateral surfaces, it is not enriched at the apical membrane during blastopore formation. Because the apical surface of bottle cells contains numerous microvilli and microfolds (Perry and Waddington, 1966; Schroeder, 1970), many apical proteins should appear to be concentrated or condensed. Therefore, it might be difficult to prove that Vangl2 accumulates in the apices of the constricted cells above the levels detected in the apices of the unconstricted cells, but this is not essential for our proposed mechanism of Vangl2 function. Of note, in deep layer ectoderm cells, Vangl2 is enriched at the lateral and the outermost surfaces, a localization that might be relevant to the potential role of Vangl2 in cell migration and intercalation. Consistent with this possibility, we observed that the ectodermal tissue depleted of Vangl2 consists of multiple cell layers by the end of gastrulation (data not shown). This differs significantly from the two-layered composition of normal ectoderm and indicates a potential defect in radial cell intercalation. Defects in epiboly (i.e. radial intercalation) have been reported previously for zebrafish embryos depleted of Celsr, another core PCP protein, but these have been attributed to Celsr function in cell adhesion rather than the PCP pathway (Carreira-Barbosa et al., 2009).

Although the significance of apical localization for Vangl2 function is currently unclear, the depletion of Vangl2 and Daam1 and interference with the function of Rock lead to the inhibition of blastopore formation and defective gastrulation. Although we observe both early and late blastopore defects in Vangl2 morphants, embryos are still able to complete gastrulation. This might be due to the incomplete depletion of Vangl2 or due to the redundant activity of Vangl1 in apical constriction at the end of gastrulation. Alternatively, a different morphogenetic process, known as convergent thickening (Keller and Danilchik, 1988), might compensate for the lack of bottle cell function during blastopore closure. This is consistent with previous work in which the microsurgical removal of bottle cells did not stop gastrulation,

Development (2015) 142, 99-107 doi:10.1242/dev.111161

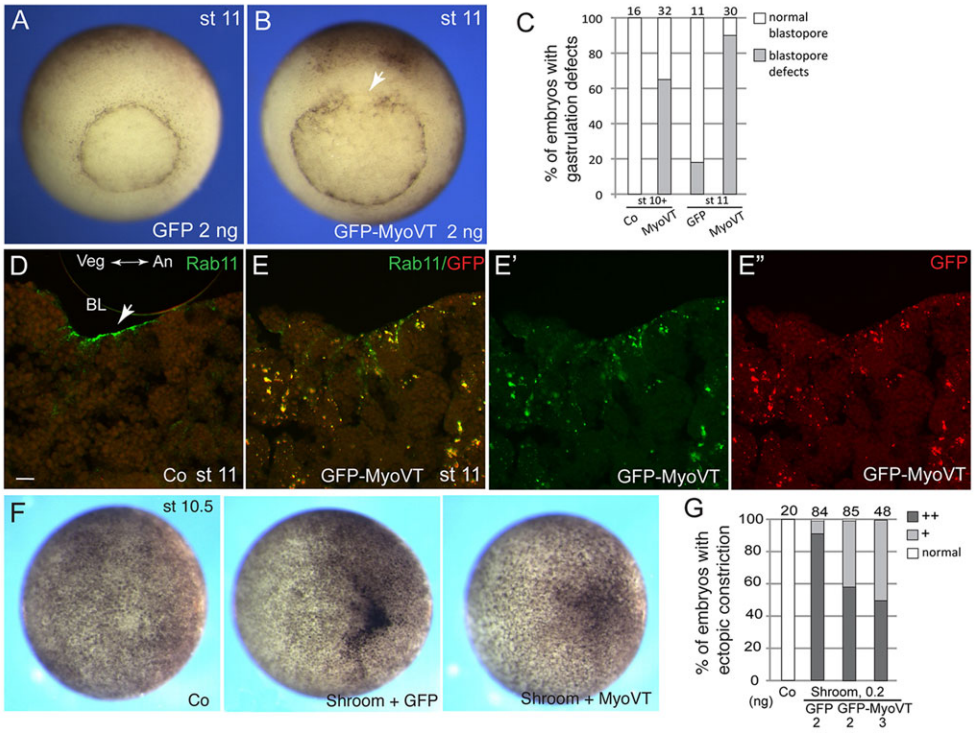

Fig. 7. Myosin V regulates endogenous and Shroom-mediated apical constriction. (A-C) Early embryos were injected with 2 ng of RNAs encoding GFP (A) or the carboxy-terminal tail of Myosin V fused to GFP (GFP-MyoVT, B). Blastopore defects of stage (st) 11 MyoVT embryos (B), as compared with the control (A) are shown. (C) Quantification of the results at the early and late gastrula stages. Co, control. (D,E) GFP-MyoVT alters the normal pattern of Rab11 distribution. BL, blastopore lip. (D) Transverse section of a stage 11 blastopore, stained for endogenous Rab11. The animal-vegetal (An-Vg) axis is indicated. Arrow points to Rab11 staining in bottle cells. Scale bar: 20 µm. (E,E″) Transverse section of a stage 11 defective blastopore from a MyoVT-expressing embryo. MyoVT forms cytoplasmic aggregates that colocalize with endogenous Rab11 protein. (F,G) GFP-MyoVT interferes with Shroom-mediated constriction. Scoring was carried out for embryos with strong (++) and mild (+) ectopic constriction.

suggesting that bottle cells assist tissue involution but are not required for blastopore closure (Hardin and Keller, 1988; Keller, 1981). Our additional experiments established that Prickle and Daam1 appear to be necessary for the ectopic apical constriction triggered by Shroom in embryonic ectoderm in the absence of mesoderm-inducing and patterning factors. Taken together, these observations establish a novel general function for PCP signaling in apical constriction. This role appears to be conserved in mammals, as indicated by the abnormal apical constriction in the neural tube of Vangl2 and Ptk7 mutant mouse embryos (Williams et al., 2014).

With respect to the underlying mechanism, we propose that Vangl2 is required for the apical accumulation of Rab11, which functions together with the motor protein Myosin V in blastopore formation. This model is consistent with the data of Lee and Harland, who reported the requirement for Rab5-dependent endocytosis in apical constriction (Lee and Harland, 2010). Whereas Rab5, a key component of the early endosome, was proposed to remove the excessive apical membrane that forms in constricting bottle cells (Lee and Harland, 2010), we demonstrate that Rab11, a component of the recycling endosome, is also required for apical constriction. Therefore, both the removal of membrane molecules from the surface and their recycling back to the cell membrane are essential for this process. As Vangl2 is dislodged from the cell membrane in Rab11 morphants, we propose that Vangl2 is one of the cargo molecules that is delivered to the cell surface by Rab11-mediated endocytic recycling. These results emphasize the significance of the positive-regulatory loop between PCP signaling and endocytic trafficking (Classen et al., 2005; Gray et al., 2009; Lee et al., 2003; Mahaffey et al., 2013).

Our data reveal a new role for vertebrate Vangl2 in epithelial folding, which is shared by several other PCP proteins. We show that a dominant-negative construct of Prickle, a Vangl2-associated PCP protein, suppresses Shroom-dependent apical constriction. Moreover, Rock and Daam1, two downstream mediators of PCP signaling, also function in the formation of bottle cells and appear to be essential for apical constriction. These results are consistent with reported delayed blastopore closure in embryos in which the functions of Daam1 and Dishevelled have been compromised (Habas et al., 2001; Sokol, 1996). Moreover, Wnt ligands and apical-basal polarity proteins that are known to interact with PCP molecules have been implicated in the same process (Choi and Sokol, 2009; Dollar et al., 2005). These observations further expand the spectrum of PCP-associated morphogenetic processes. Besides planar epithelial polarity, PCP proteins were reported to affect mitotic spindle orientation and cell differentiation (Bellaiche et al., 2004; Cortijo et al., 2012; Lake and Sokol, 2009), cilia positioning (Hashimoto et al., 2010; Song et al., 2010), axon guidance (Lyuksyutova et al., 2003; Tissir and Goffinet, 2013), apical-basal polarity (Tao et al., 2009), oocyte development (Cha et al., 2011) and migration of endodermal (Trichas et al., 2012), germ cell (Laird et al., 2011) and neuronal progenitors (Carreira-Barbosa et al., 2003; Glasco et al., 2012; Jessen et al., 2002). Additionally, Vangl2 and Rock are involved in lung branching morphogenesis (Yates et al., 2010b), and both Vangl2 and Daam1 were reported to function in kidney tubulogenesis (Miller et al., 2011; Yates et al., 2010a). Whereas Wnt/Frizzled signaling was proposed to directly control endodermal cell ingression in *Caenorhabditis elegans* (Lee et al., 2006), mutations in the worm VANG-1 and FMI-1/Celsr homologs do not reveal gastrulation phenotypes (Sawa, 2012). Thus, it is currently unclear whether the proposed function of Vangl2 in apical constriction is conserved in invertebrates.

The involvement of Vangl2 in apical constriction differs from the known functions of PCP proteins in cell intercalations and in coordinating the orientation of a cell relative to its neighbors (Gray et al., 2011; Keller, 2002; Sokol, 2000; Wallingford, 2012). This multi-functionality of Vangl2 resembles the pleiotropic roles of actomyosin complexes, which function in different cellular compartments to mediate diverse cell behaviors (Heisenberg and Bellaiche, 2013; Tada and Kai, 2012). Although the number of

Development (2015) 142, 99-107 doi:10.1242/dev.111161

molecular players is limited, their specific interactions in a certain location within a cell must be crucial for the signaling outcome, such as the decision to migrate or to constrict the apical surface of the cell. Defining the molecular pathways controlling cell behavior will remain a major challenge for future studies of morphogenesis.

One possibility is that Wnt/PCP proteins directly modulate Myosin II activation and apical constriction through Rho-associated kinase (Marlow et al., 2002; Shindo and Wallingford, 2014; Winter et al., 2001) and one of the RhoGEFs, such as PDZ-RhoGEF (Nishimura et al., 2012) or GEF-H1, a RhoGEF that triggers ectopic apical constriction (Itoh et al., 2014). Consistent with this idea, we observed a decrease in MLC phosphorylation at the blastopore in Vangl2-depleted embryos. Although Vangl2 activity has been associated with the regulation of adherens junctions (Lindqvist et al., 2010), the direct link between Vangl2 and Rock or Myosin activation remains to be established. Alternatively, the Wnt/PCP pathway might modulate Myosin II activity in bottle cells through Rab11-mediated trafficking. The ability of overexpressed Rab11 to rescue blastopore defects in Vangl2-depleted embryos suggests that vesicular trafficking plays an essential role in PCP signaling during blastopore formation. The apical enrichment of PCP proteins in the blastopore cells might relate to the known functions of Rab11 and Myosin V in apical recycling in tissue culture cells (Bryant et al., 2010; Li et al., 2007; Roland et al., 2011). We note that apical protein localization has been previously associated with PCP signaling due to the apical distribution of Frizzled in *Drosophila* wing cells (Wu et al., 2004). Moreover, apical PCP protein distribution has been observed in the mouse node cells (Antic et al., 2010; Hashimoto et al., 2010; Mahaffey et al., 2013). Based on the effect of Vangl2 MO on Rab11 localization, we propose that PCP signaling plays a general role in apical constriction by targeting Rab11-positive recycling endosomes within the apical compartment. This hypothesis is supported by other studies implicating PCP components in the control of membrane dynamics and vesicular trafficking in *Drosophila* and vertebrates (Classen et al., 2005; Gray et al., 2009; Lee et al., 2003; Mahaffey et al., 2013). Although many molecules can serve as a cargo for Rab11 recycling vesicles, one possibility is that PCP proteins themselves are recycled to the cell surface to act at the site of apical constriction (Devenport et al., 2011). Our observations support a positive-feedback model in which PCP signaling and endocytic trafficking cooperatively function during apical constriction.

MATERIALS AND METHODS

Plasmids, mRNA synthesis and morpholinos

The plasmids encoding CFP-Vangl2/Stbm (Itoh et al., 2009), mouse HA-Vangl2 (Gao et al., 2011), mouse Shroom/ShrmL (also known as Shroom3) (Hildebrand and Soriano, 1999) and mouse FLAG-Shroom (Plageman et al., 2010; Chu et al., 2013) in pCS2 were as described previously. Zebrafish Prickle1a cDNA was provided by M. Tada (University College London, UK). The PET and LIM domains were removed in the zPk1ΔPL mutant by PCR-based mutagenesis. Other constructs were N-Daam1-pCS2+ (Habas et al., 2001), myc-DN-ROCK-pCS2 (Marlow et al., 2002) and pRK5myc RhoA-N19 (a gift from A. Hall, Memorial Sloan Kettering Cancer Center, New York, USA). *Xenopus* Rab11 constructs were as described previously (Kim et al., 2012). GFP-MyoVT-pCS2 was created by subcloning the insert from the original construct (Lapierre et al., 2001).

Capped mRNAs were made by *in vitro* transcription from the T7 or SP6 promoters using mMessage mMachine kit (Ambion). Cytoplasmic GFP (50-100 pg) RNA was co-injected with MOs or RNAs as a lineage tracer. The Rab11 MO (5′-TACCCATCGTCGCGGCACTTCTGAC-3′) (Kim et al., 2012) and Vangl2/Stbm MO (Darken et al., 2002) were as described previously. The sequence of the control MO was 5′-GCTTCAGCTAGTGACACATGCAT-3′ (Itoh et al., 2014). The Daam1 MO sequence was 5′-GGCCATGGCCGCAGGTCTGTCAGTT-3′.

Xenopus embryos, RNA injections and apical constriction

In vitro fertilization, culture and staging of *Xenopus laevis* embryos were carried out as described previously (Dollar et al., 2005). For microinjections, four-cell embryos were transferred into 2% Ficoll in 0.3×MMR buffer, and 5 nl of mRNAs or MO solution was injected into one or more blastomeres. Amounts of injected mRNA or MO per embryo have been optimized in preliminary dose-response experiments (data not shown) and are indicated in figure legends. For ectopic apical constriction, four- to eight-cell embryos were injected animally into one dorsal and one ventral animal blastomere. Embryonic defects were scored as the percentage of embryos with the representative phenotype, based on three to five independent experiments. Each experimental group contained 25-35 embryos.

Immunohistochemistry and immunoblot analysis

Anti-Vangl2 antibodies were generated by immunizing rabbits with the peptide corresponding to amino acids 56-70 of *Xenopus* Vangl2 and affinity-purified on a column with the covalently bound peptide. The 60 kDa Vangl2 band recognized by this antibody in *Xenopus* gastrula stage lysates was depleted in Vangl2 morphants (data not shown). The initial characterization of Vangl2 protein localization was performed using anti-Vangl2 antibodies provided by M. Montcouquiol (Université Bordeaux, France).

For cryosectioning, the embryos were embedded in solution containing 15% cold fish gelatin and 15% sucrose, sectioned at 10 µm and immunostained overnight, essentially as described previously (Dollar et al., 2005). Antibodies against the following antigens were used: Vangl2 [1:100, rabbit polyclonal, a gift from M. Montcouquiol (Montcouquiol et al., 2006); and this study, 1:100, rabbit polyclonal], Rab11 (1:100, Zymed, rabbit monoclonal; 1:100, Invitrogen, rabbit polyclonal; and 1:100, BD Biosciences, mouse monoclonal), GFP (1:200; B-2, Santa Cruz Biotechnology, mouse; or Invitrogen, rabbit), anti-phospho-Ser20 myosin light chain (anti-pMLC, 1:300; Abcam, rabbit), β1-integrin (1:50; 8C8, Dollar et al., 2005, mouse monoclonal). Secondary antibodies were against mouse or rabbit IgG conjugated to Alexa Fluor 488, Alexa Fluor 555 (1:100, Invitrogen) or Cy3 (1:100, Jackson ImmunoResearch). Cryosections were mounted for observation with the Vectashield mounting medium (Vector). For detection of Rab11 and pMLC on cryosections, embryos were devitellinized, fixed with 2% trichloroacetic acid (TCA) solution for 30 min at room temperature and washed with 0.3% Triton X-100 in PBS for 30 min (Nandadasa et al., 2009). Standard specificity controls were performed to confirm lack of crossreactivity and no staining without primary antibodies. Immunofluorescence images were captured using the Axio Imager fluorescence microscope (Zeiss) and the AxioVision imaging software (Zeiss). Results are shown as representative images from at least three independent experiments, each containing 10-20 embryos per group.

For *en face* immunofluorescent imaging of the blastopore lip, stage 10+ embryos injected with control MO or Vangl2 MO with GFP RNA as a tracer were devitellinized, fixed for 1 h with MEMFA (0.1 M MOPS pH 7.4, 2 mM EGTA, 1 mM $MgSO_4$ and 3.7% formaldehyde), washed with PBS and subjected to whole-mount immunostaining. Samples were blocked with 10% goat serum in PBS for 1 h at room temperature. For F-actin visualization, fixed embryos were co-stained with phalloidin conjugated to Alexa Fluor 568 (5 units/ml, Molecular Probes) and anti-GFP antibodies (1:200, B-2, Santa Cruz mouse monoclonal) overnight at 4°C in 10% goat serum in PBS. After washing, samples were incubated with anti-mouse-IgG secondary antibodies conjugated to Alexa Fluor 488 (Molecular Probes, 1:500) for 2 h in 10% goat serum in PBS. After washing, dorsal lip explants were dissected with a razor blade and mounted for observation in the Vectashield mounting medium (Vector).

Western blot analysis was carried out as described previously (Ossipova et al., 2009). Briefly, whole embryos or animal cap explants were lysed in a buffer containing 1% Triton X-100, 50 mM sodium chloride, 50 mM Tris-HCl pH 7.6, 1 mM EDTA, 0.6 mM phenylmethylsulphonyl fluoride (PMSF), 10 mM sodium fluoride and 1 mM sodium orthovanadate. The lysates were subjected to SDS-polyacrylamide gel electrophoresis, and proteins were transferred to a PVDF membrane for immunodetection with rabbit polyclonal anti-Vangl2 antibody (Montcouquiol et al., 2006; and this study).

Development (2015) 142, 99-107 doi:10.1242/dev.111161

RT-PCR analysis

Total RNA was extracted from stage 10.5 embryos using an RNeasy kit (Qiagen) according to the manufacturer's instructions. cDNAs were made from DNase-treated RNA using the Superscript first-strand synthesis system (Invitrogen). The RT-PCR primers were as follows: *Gsc* forward, 5′-GAACAGCTGGCAAGGAGAGT-3; and *Gsc* reverse, 5′-GATCTTTCTGCCTCCTCCA-3′; *Odc* forward, 5′-CATCTTTCACCCTGGCAGTT-3′; and *Odc* reverse, 5′-CATTGGCAGCATCTTCTTCA-3′; *Gef3.2* (GenBank accession number NM_001096674.1) forward, 5′-AGTGGGTTTCAAAAATGGAT-3′; and *Gef3.2* reverse, 5′-CTTTCAACCTCCTCCTTGTT-3′. The primers for other genes, including *Chordin* (Hikasa and Sokol, 2004), *FoxD3* (Ossipova et al., 2011) and *Xbra* (Agius et al., 2000), were as described previously.

The number of PCR cycles for each primer pair was determined empirically to maintain amplification in the linear range. One quarter of each PCR reaction was electrophoresed in 2% agarose gel, stained with ethidium bromide and photographed under ultraviolet light.

Acknowledgements

We thank J. Goldenring, R. Habas, A. Hall, R. Lang, F. Marlow, P. Soriano, Y. Yang and M. Tada for plasmids, M. Montcouquiol and J. Ezan for anti-Vangl2 antibodies, and B. Lake for the initial experiments with Rab11. We also thank members of the Sokol laboratory for discussions.

Competing interests

The authors declare no competing financial interests.

Author contributions

O.O. and S.Y.S. designed the experiments and wrote the manuscript. O.O. performed the experiments. I.C. designed and analyzed RT-PCR experiments, C.-W.C. generated and tested the zPk1ΔPL construct. All authors edited the manuscript.

Funding

This study was supported by National Institutes of Health grants [NS40972 and HD078874 to S.Y.S.]. Deposited in PMC for release after 12 months.

Supplementary material

Supplementary material available online at
http://dev.biologists.org/lookup/suppl/doi:10.1242/dev.111161/-/DC1

References

Agius, E., Oelgeschlager, M., Wessely, O., Kemp, C. and De Robertis, E. M. (2000). Endodermal Nodal-related signals and mesoderm induction in Xenopus. *Development* **127**, 1173-1183.

Antic, D., Stubbs, J. L., Suyama, K., Kintner, C., Scott, M. P. and Axelrod, J. D. (2010). Planar cell polarity enables posterior localization of nodal cilia and left-right axis determination during mouse and Xenopus embryogenesis. *PLoS ONE* **5**, pe8999.

Axelrod, J. D. (2009). Progress and challenges in understanding planar cell polarity signaling. *Semin. Cell Dev. Biol.* **20**, 964-971.

Bastock, R., Strutt, H. and Strutt, D. (2003). Strabismus is asymmetrically localised and binds to Prickle and Dishevelled during Drosophila planar polarity patterning. *Development* **130**, 3007-3014.

Bellaïche, Y., Beaudoin-Massiani, O., Stüttem, I. and Schweisguth, F. (2004). The planar cell polarity protein Strabismus promotes Pins anterior localization during asymmetric division of sensory organ precursor cells in Drosophila. *Development* **131**, 469-478.

Borovina, A., Superina, S., Voskas, D. and Ciruna, B. (2010). Vangl2 directs the posterior tilting and asymmetric localization of motile primary cilia. *Nat. Cell Biol.* **12**, 407-412.

Bryant, D. M., Datta, A., Rodríguez-Fraticelli, A. E., Peränen, J., Martín-Belmonte, F. and Mostov, K. E. (2010). A molecular network for de novo generation of the apical surface and lumen. *Nat. Cell Biol.* **12**, 1035-1045.

Carreira-Barbosa, F., Concha, M. L., Takeuchi, M., Ueno, N., Wilson, S. W. and Tada, M. (2003). Prickle 1 regulates cell movements during gastrulation and neuronal migration in zebrafish. *Development* **130**, 4037-4046.

Carreira-Barbosa, F., Kajita, M., Morel, V., Wada, H., Okamoto, H., Martinez Arias, A., Fujita, Y., Wilson, S. W. and Tada, M. (2009). Flamingo regulates epiboly and convergence/extension movements through cell cohesive and signalling functions during zebrafish gastrulation. *Development* **136**, 383-392.

Carroll, T. J. and Yu, J. (2012). The kidney and planar cell polarity. *Curr. Top. Dev. Biol.* **101**, 185-212.

Cha, S.-W., Tadjuidje, E., Wylie, C. and Heasman, J. (2011). The roles of maternal Vangl2 and aPKC in Xenopus oocyte and embryo patterning. *Development* **138**, 3989-4000.

Choi, S.-C. and Sokol, S. Y. (2009). The involvement of lethal giant larvae and Wnt signaling in bottle cell formation in Xenopus embryos. *Dev. Biol.* **336**, 68-75.

Chu, C. W., Gerstenzang, E., Ossipova, O. and Sokol, S. Y. (2013). Lulu regulates Shroom-induced apical constriction during neural tube closure. *PLoS One* **8**, e81854.

Classen, A.-K., Anderson, K. I., Marois, E. and Eaton, S. (2005). Hexagonal packing of Drosophila wing epithelial cells by the planar cell polarity pathway. *Dev. Cell* **9**, 805-817.

Copp, A. J. and Greene, N. D. (2010). Genetics and development of neural tube defects. *J. Pathol.* **220**, 217-230.

Cortijo, C., Gouzi, M., Tissir, F. and Grapin-Botton, A. (2012). Planar cell polarity controls pancreatic beta cell differentiation and glucose homeostasis. *Cell Rep.* **2**, 1593-1606.

Darken, R. S., Scola, A. M., Rakeman, A. S., Das, G., Mlodzik, M. and Wilson, P. A. (2002). The planar polarity gene strabismus regulates convergent extension movements in Xenopus. *EMBO J.* **21**, 976-985.

Devenport, D., Oristian, D., Heller, E. and Fuchs, E. (2011). Mitotic internalization of planar cell polarity proteins preserves tissue polarity. *Nat. Cell Biol.* **13**, 893-902.

Dollar, G. L., Weber, U., Mlodzik, M. and Sokol, S. Y. (2005). Regulation of Lethal giant larvae by Dishevelled. *Nature* **437**, 1376-1380.

Gao, B., Song, H., Bishop, K., Elliot, G., Garrett, L., English, M. A., Andre, P., Robinson, J., Sood, R., Minami, Y. et al. (2011). Wnt signaling gradients establish planar cell polarity by inducing Vangl2 phosphorylation through Ror2. *Dev. Cell* **20**, 163-176.

Glasco, D. M., Sittaramane, V., Bryant, W., Fritzsch, B., Sawant, A., Paudyal, A., Stewart, M., Andre, P., Cadete Vilhais-Neto, G., Yang, Y. et al. (2012). The mouse Wnt/PCP protein Vangl2 is necessary for migration of facial branchiomotor neurons, and functions independently of Dishevelled. *Dev. Biol.* **369**, 211-222.

Gray, R. S., Abitua, P. B., Wlodarczyk, B. J., Szabo-Rogers, H. L., Blanchard, O., Lee, I., Weiss, G. S., Liu, K. J., Marcotte, E. M., Wallingford, J. B. et al. (2009). The planar cell polarity effector Fuz is essential for targeted membrane trafficking, ciliogenesis and mouse embryonic development. *Nat. Cell Biol.* **11**, 1225-1232.

Gray, R. S., Roszko, I. and Solnica-Krezel, L. (2011). Planar cell polarity: coordinating morphogenetic cell behaviors with embryonic polarity. *Dev. Cell* **21**, 120-133.

Gubb, D. and Garcia-Bellido, A. (1982). A genetic analysis of the determination of cuticular polarity during development in Drosophila melanogaster. *J. Embryol. Exp. Morphol.* **68**, 37-57.

Habas, R., Kato, Y. and He, X. (2001). Wnt/Frizzled activation of Rho regulates vertebrate gastrulation and requires a novel Formin homology protein Daam1. *Cell* **107**, 843-854.

Haigo, S. L., Hildebrand, J. D., Harland, R. M. and Wallingford, J. B. (2003). Shroom induces apical constriction and is required for hingepoint formation during neural tube closure. *Curr. Biol.* **13**, 2125-2137.

Hardin, J. and Keller, R. (1988). The behaviour and function of bottle cells during gastrulation of Xenopus laevis. *Development* **103**, 211-230.

Harland, R. and Gerhart, J. (1997). Formation and function of Spemann's organizer. *Annu. Rev. Cell Dev. Biol.* **13**, 611-667.

Hashimoto, M., Shinohara, K., Wang, J., Ikeuchi, S., Yoshiba, S., Meno, C., Nonaka, S., Takada, S., Hatta, K., Wynshaw-Boris, A. et al. (2010). Planar polarization of node cells determines the rotational axis of node cilia. *Nat. Cell Biol.* **12**, 170-176.

Heisenberg, C.-P. and Bellaïche, Y. (2013). Forces in tissue morphogenesis and patterning. *Cell* **153**, 948-962.

Hikasa, H. and Sokol, S. Y. (2004). The involvement of Frodo in TCF-dependent signaling and neural tissue development. *Development* **131**, 4725-4734.

Hildebrand, J. D. and Soriano, P. (1999). Shroom, a PDZ domain-containing actin-binding protein, is required for neural tube morphogenesis in mice. *Cell* **99**, 485-497.

Itoh, K., Jenny, A., Mlodzik, M. and Sokol, S. Y. (2009). Centrosomal localization of Diversin and its relevance to Wnt signaling. *J. Cell Sci.* **122**, 3791-3798.

Itoh, K., Ossipova, O. and Sokol, S. Y. (2014). GEF-H1 functions in apical constriction and cell intercalations and is essential for vertebrate neural tube closure. *J. Cell Sci.* **127**, 2542–2553.

Jenny, A., Reynolds-Kenneally, J., Das, G., Burnett, M. and Mlodzik, M. (2005). Diego and Prickle regulate Frizzled planar cell polarity signalling by competing for Dishevelled binding. *Nat. Cell Biol.* **7**, 691-697.

Jessen, J. R., Topczewski, J., Bingham, S., Sepich, D. S., Marlow, F., Chandrasekhar, A. and Solnica-Krezel, L. (2002). Zebrafish trilobite identifies new roles for Strabismus in gastrulation and neuronal movements. *Nat. Cell Biol.* **4**, 610-615.

Ju, R., Cirone, P., Lin, S., Griesbach, H., Slusarski, D. C. and Crews, C. M. (2010). Activation of the planar cell polarity formin DAAM1 leads to inhibition of endothelial cell proliferation, migration, and angiogenesis. *Proc. Natl. Acad. Sci. USA* **107**, 6906-6911.

Keller, R. E. (1981). An experimental analysis of the role of bottle cells and the deep marginal zone in gastrulation of Xenopus laevis. *J. Exp. Zool.* **216**, 81-101.

Keller, R. (2002). Shaping the vertebrate body plan by polarized embryonic cell movements. *Science* **298**, 1950-1954.
Keller, R. and Danilchik, M. (1988). Regional expression, pattern and timing of convergence and extension during gastrulation of Xenopus laevis. *Development* **103**, 193-209.
Kim, K., Lake, B. B., Haremaki, T., Weinstein, D. C. and Sokol, S. Y. (2012). Rab11 regulates planar polarity and migratory behavior of multiciliated cells in Xenopus embryonic epidermis. *Dev. Dyn.* **241**, 1385-1395.
Laird, D. J., Altshuler-Keylin, S., Kissner, M. D., Zhou, X. and Anderson, K. V. (2011). Ror2 enhances polarity and directional migration of primordial germ cells. *PLoS Genet.* **7**, pe1002428.
Lake, B. B. and Sokol, S. Y. (2009). Strabismus regulates asymmetric cell divisions and cell fate determination in the mouse brain. *J. Cell Biol.* **185**, 59-66.
Lapierre, L. A., Kumar, R., Hales, C. M., Navarre, J., Bhartur, S. G., Burnette, J. O., Provance, D. W.Jr, Mercer, J. A., Bahler, M. and Goldenring, J. R. (2001). Myosin vb is associated with plasma membrane recycling systems. *Mol. Biol. Cell* **12**, 1843-1857.
Lee, J.-Y. and Harland, R. M. (2007). Actomyosin contractility and microtubules drive apical constriction in Xenopus bottle cells. *Dev. Biol.* **311**, 40-52.
Lee, J.-Y. and Harland, R. M. (2010). Endocytosis is required for efficient apical constriction during Xenopus gastrulation. *Curr. Biol.* **20**, 253-258.
Lee, O.-K., Frese, K. K., James, J. S., Chadda, D., Chen, Z.-H., Javier, R. T. and Cho, K.-O. (2003). Discs-Large and Strabismus are functionally linked to plasma membrane formation. *Nat. Cell Biol.* **5**, 987-993.
Lee, J.-Y., Marston, D. J., Walston, T., Hardin, J., Halberstadt, A. and Goldstein, B. (2006). Wnt/Frizzled signaling controls C. elegans gastrulation by activating actomyosin contractility. *Curr. Biol.* **16**, 1986-1997.
Li, B. X., Satoh, A. K. and Ready, D. F. (2007). Myosin V, Rab11, and dRip11 direct apical secretion and cellular morphogenesis in developing Drosophila photoreceptors. *J. Cell Biol.* **177**, 659-669.
Lindqvist, M., Horn, Z., Bryja, V., Schulte, G., Papachristou, P., Ajima, R., Dyberg, C., Arenas, E., Yamaguchi, T. P., Lagercrantz, H. et al. (2010). Vang-like protein 2 and Rac1 interact to regulate adherens junctions. *J. Cell Sci.* **123**, 472-483.
Lyuksyutova, A. I., Lu, C.-C., Milanesio, N., King, L. A., Guo, N., Wang, Y., Nathans, J., Tessier-Lavigne, M. and Zou, Y. (2003). Anterior-posterior guidance of commissural axons by Wnt-frizzled signaling. *Science* **302**, 1984-1988.
Mahaffey, J. P., Grego-Bessa, J., Liem, K. F.Jr and Anderson, K. V. (2013). Cofilin and Vangl2 cooperate in the initiation of planar cell polarity in the mouse embryo. *Development* **140**, 1262-1271.
Marlow, F., Topczewski, J., Sepich, D. and Solnica-Krezel, L. (2002). Zebrafish Rho kinase 2 acts downstream of Wnt11 to mediate cell polarity and effective convergence and extension movements. *Curr. Biol.* **12**, 876-884.
Miller, R. K., de la Torre Canny, S. G., Jang, C.-W., Cho, K., Ji, H., Wagner, D. S., Jones, E. A., Habas, R. and McCrea, P. D. (2011). Pronephric tubulogenesis requires Daam1-mediated planar cell polarity signaling. *J. Am. Soc. Nephrol.* **22**, 1654-1664.
Mizuno-Yamasaki, E., Rivera-Molina, F. and Novick, P. (2012). GTPase networks in membrane traffic. *Annu. Rev. Biochem.* **81**, 637-659.
Montcouquiol, M., Rachel, R. A., Lanford, P. J., Copeland, N. G., Jenkins, N. A. and Kelley, M. W. (2003). Identification of Vangl2 and Scrb1 as planar polarity genes in mammals. *Nature* **423**, 173-177.
Montcouquiol, M., Sans, N., Huss, D., Kach, J., Dickman, J. D., Forge, A., Rachel, R. A., Copeland, N. G., Jenkins, N. A., Bogani, D. et al. (2006). Asymmetric localization of Vangl2 and Fz3 indicate novel mechanisms for planar cell polarity in mammals. *J. Neurosci.* **26**, 5265-5275.
Nandadasa, S., Tao, Q., Menon, N. R., Heasman, J. and Wylie, C. (2009). N- and E-cadherins in Xenopus are specifically required in the neural and non-neural ectoderm, respectively, for F-actin assembly and morphogenetic movements. *Development* **136**, 1327-1338.
Nishimura, T., Honda, H. and Takeichi, M. (2012). Planar cell polarity links axes of spatial dynamics in neural-tube closure. *Cell* **149**, 1084-1097.
Ossipova, O., Ezan, J. and Sokol, S. Y. (2009). PAR-1 phosphorylates Mind bomb to promote vertebrate neurogenesis. *Dev. Cell* **17**, 222-233.
Ossipova, O. and Sokol, S. Y. (2011). Neural crest specification by noncanonical Wnt signaling and PAR-1. *Development* **138**, 5441-5450.
Ossipova, O., Kim, K., Lake, B. B., Itoh, K., Ioannou, A. and Sokol, S. Y. (2014). Role of Rab11 in planar cell polarity and apical constriction during vertebrate neural tube closure. *Nat. Commun.* **5**, 3734.
Perry, M. M. and Waddington, C. H. (1966). Ultrastructure of the blastopore cells in the newt. *J. Embryol. Exp. Morphol.* **15**, 317-330.
Plageman, T. F., Jr, Chung, M.-I., Lou, M., Smith, A. N., Hildebrand, J. D., Wallingford, J. B. and Lang, R. A. (2010). Pax6-dependent Shroom3 expression regulates apical constriction during lens placode invagination. *Development* **137**, 405-415.
Roland, J. T., Bryant, D. M., Datta, A., Itzen, A., Mostov, K. E. and Goldenring, J. R. (2011). Rab GTPase-Myo5B complexes control membrane recycling and epithelial polarization. *Proc. Natl. Acad. Sci. USA* **108**, 2789-2794.
Sawa, H. (2012). Control of cell polarity and asymmetric division in C. elegans. *Curr. Top. Dev. Biol.* **101**, 55-76.
Sawyer, J. M., Harrell, J. R., Shemer, G., Sullivan-Brown, J., Roh-Johnson, M. and Goldstein, B. (2010). Apical constriction: a cell shape change that can drive morphogenesis. *Dev. Biol.* **341**, 5-19.
Schroeder, T. E. (1970). Neurulation in Xenopus laevis. An analysis and model based upon light and electron microscopy. *J. Embryol. Exp. Morphol.* **23**, 427-462.
Shindo, A. and Wallingford, J. B. (2014). PCP and septins compartmentalize cortical actomyosin to direct collective cell movement. *Science* **343**, 649-652.
Sokol, S. Y. (1996). Analysis of Dishevelled signalling pathways during Xenopus development. *Curr. Biol.* **6**, 1456-1467.
Sokol, S. (2000). A role for Wnts in morpho-genesis and tissue polarity. *Nat. Cell Biol.* **2**, E124-E125.
Song, H., Hu, J., Chen, W., Elliott, G., Andre, P., Gao, B. and Yang, Y. (2010). Planar cell polarity breaks bilateral symmetry by controlling ciliary positioning. *Nature* **466**, 378-382.
Tada, M. and Kai, M. (2012). Planar cell polarity in coordinated and directed movements. *Curr. Top. Dev. Biol.* **101**, 77-110.
Takeuchi, M., Nakabayashi, J., Sakaguchi, T., Yamamoto, T. S., Takahashi, H., Takeda, H. and Ueno, N. (2003). The prickle-related gene in vertebrates is essential for gastrulation cell movements. *Curr. Biol.* **13**, 674-679.
Tao, H., Suzuki, M., Kiyonari, H., Abe, T., Sasaoka, T. and Ueno, N. (2009). Mouse prickle1, the homolog of a PCP gene, is essential for epiblast apical-basal polarity. *Proc. Natl. Acad. Sci. USA* **106**, 14426-14431.
Tissir, F. and Goffinet, A. M. (2013). Shaping the nervous system: role of the core planar cell polarity genes. *Nat. Rev. Neurosci.* **14**, 525-535.
Tree, D. R. P., Ma, D. and Axelrod, J. D. (2002a). A three-tiered mechanism for regulation of planar cell polarity. *Semin. Cell Dev. Biol.* **13**, 217-224.
Tree, D. R. P., Shulman, J. M., Rousset, R., Scott, M. P., Gubb, D. and Axelrod, J. D. (2002b). Prickle mediates feedback amplification to generate asymmetric planar cell polarity signaling. *Cell* **109**, 371-381.
Trichas, G., Smith, A. M., White, N., Wilkins, V., Watanabe, T., Moore, A., Joyce, B., Sugnaseelan, J., Rodriguez, T. A., Kay, D. et al. (2012). Multi-cellular rosettes in the mouse visceral endoderm facilitate the ordered migration of anterior visceral endoderm cells. *PLoS Biol.* **10**, pe1001256.
Vinson, C. R. and Adler, P. N. (1987). Directional non-cell autonomy and the transmission of polarity information by the frizzled gene of Drosophila. *Nature* **329**, 549-551.
Wallingford, J. B. (2012). Planar cell polarity and the developmental control of cell behavior in vertebrate embryos. *Annu. Rev. Cell Dev. Biol.* **28**, 627-653.
Wang, Y. and Nathans, J. (2007). Tissue/planar cell polarity in vertebrates: new insights and new questions. *Development* **134**, 647-658.
Williams, M., Yen, W., Lu, X. and Sutherland, A. (2014). Distinct apical and basolateral mechanisms drive planar cell polarity-dependent convergent extension of the mouse neural plate. *Dev. Cell* **29**, 34-46.
Winter, C. G., Wang, B., Ballew, A., Royou, A., Karess, R., Axelrod, J. D. and Luo, L. (2001). Drosophila Rho-associated kinase (Drok) links Frizzled-mediated planar cell polarity signaling to the actin cytoskeleton. *Cell* **105**, 81-91.
Wu, J. and Mlodzik, M. (2008). The frizzled extracellular domain is a ligand for Van Gogh/Stbm during nonautonomous planar cell polarity signaling. *Dev. Cell* **15**, 462-469.
Wu, X., Bowers, B., Rao, K., Wei, Q. and Hammer, J. A., III. (1998). Visualization of melanosome dynamics within wild-type and dilute melanocytes suggests a paradigm for myosin V function In vivo. *J. Cell Biol.* **143**, 1899-1918.
Wu, J., Klein, T. J. and Mlodzik, M. (2004). Subcellular localization of frizzled receptors, mediated by their cytoplasmic tails, regulates signaling pathway specificity. *PLoS Biol.* **2**, pE158.
Yates, L. L., Papakrivopoulou, J., Long, D. A., Goggolidou, P., Connolly, J. O., Woolf, A. S. and Dean, C. H. (2010a). The planar cell polarity gene Vangl2 is required for mammalian kidney-branching morphogenesis and glomerular maturation. *Hum. Mol. Genet.* **19**, 4663-4676.
Yates, L. L., Schnatwinkel, C., Murdoch, J. N., Bogani, D., Formstone, C. J., Townsend, S., Greenfield, A., Niswander, L. A. and Dean, C. H. (2010b). The PCP genes Celsr1 and Vangl2 are required for normal lung branching morphogenesis. *Hum. Mol. Genet.* **19**, 2251-2267.

Supplementary information

Supplementary figure legends to Figures S1-S5.

Fig. S1

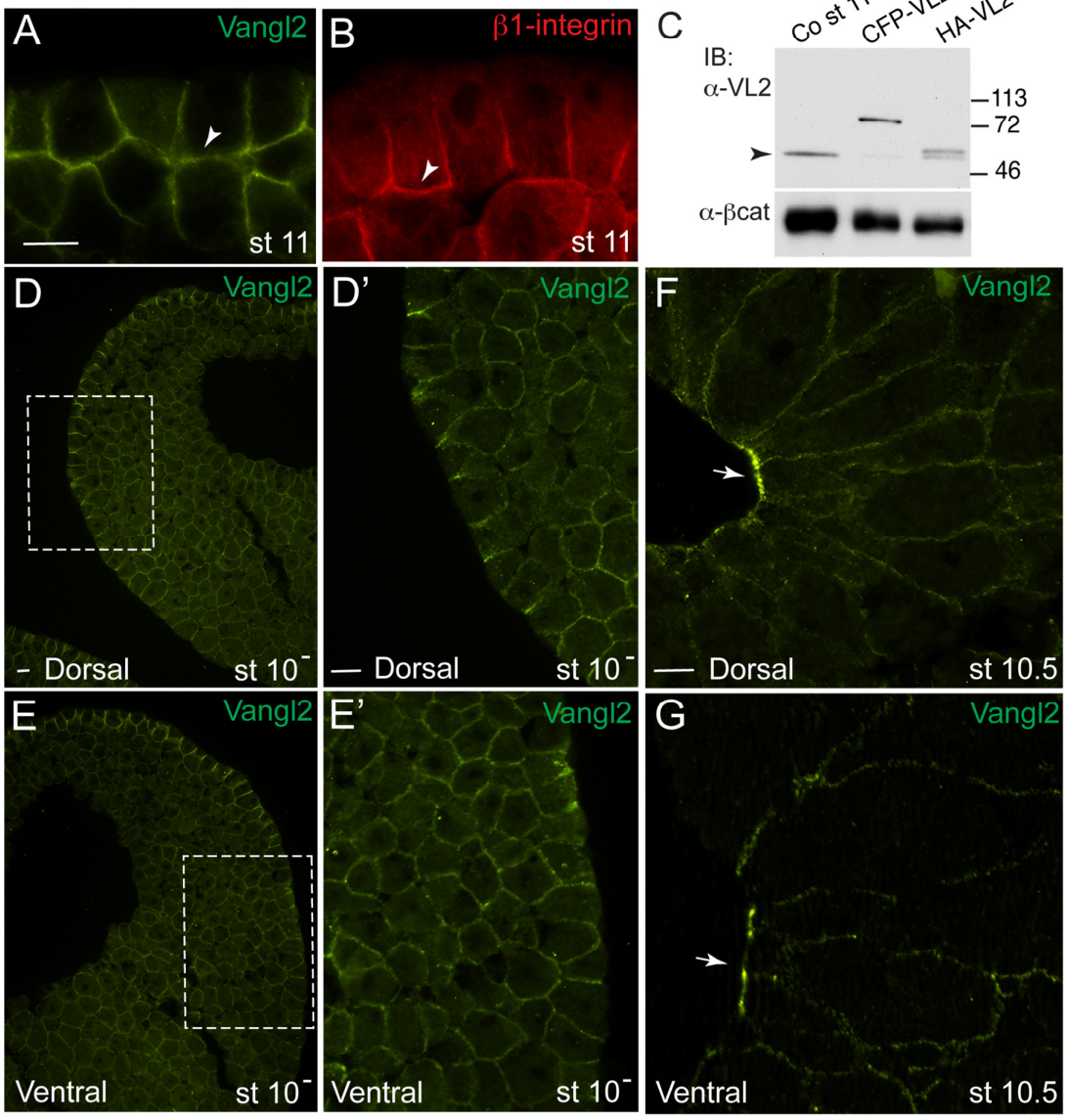

Fig. S1. Immunodetection of endogenous Vangl2 protein.

(A, B) Basolateral localization (arrowhead) of Vangl2 (A) and β1-integrin (B) in embryonic ectoderm at stage 11. (C) Immunoblot of ectodermal cell lysates with anti-Vangl2 antibody reveals a 60 kDa band (arrowhead) corresponding to endogenous Vangl2, misexpressed *Xenopus* CFP-Vangl2 and mouse HA-VL2, as indicated.

(D-G) Vangl2 immunostaining on cross-sections of st. 10^{-} and st. 10.5 embryos. Dashed boxes in D and E correspond to the magnified images shown in D' and E'. Vangl2 is detected at the basolateral membrane and in cytoplasmic vesicles near the apical cortex, and appears more abundant in the superficial cell layer. Scale bar in A is 20 μm. Both apical (arrow) and basolateral staining is detected in the constricting blastopore cells of st. 10.5 embryo. D-G, Scale bar is 20 μm.

Fig. S2

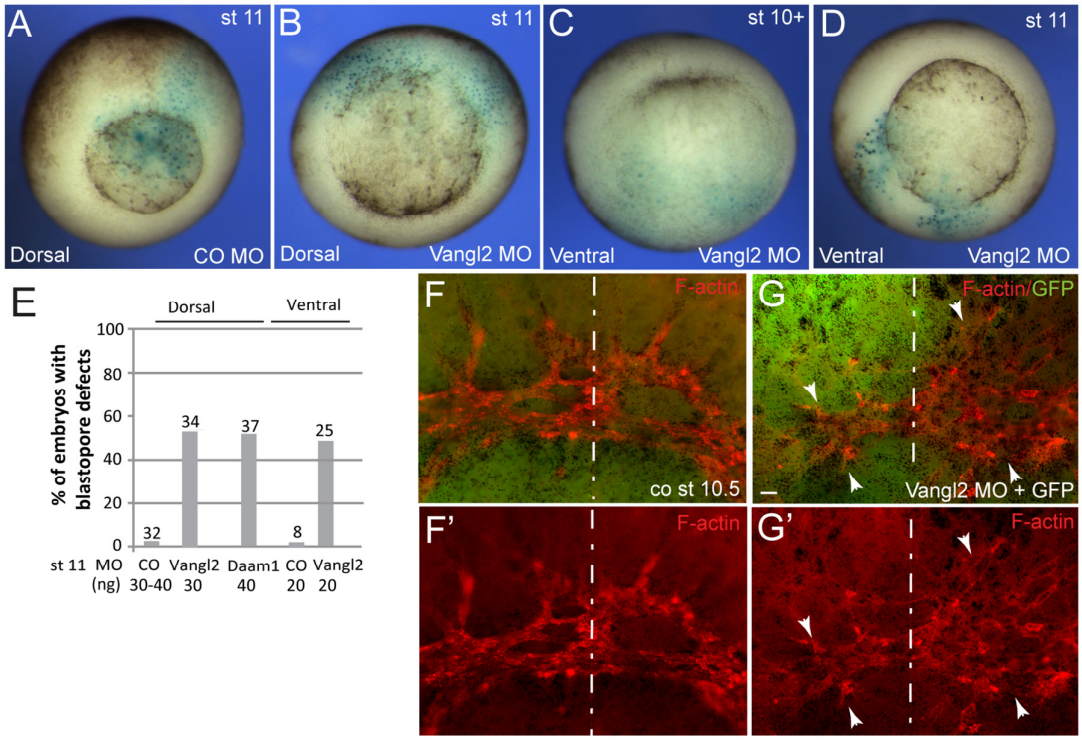

Fig. S2. Inhibition of blastopore lip formation in Vangl2-depleted embryos. (A-E) Early embryos were injected with Vangl2 MO or control MO either dorsally or ventrally as indicated. LacZ RNA (150 pg) has been coinjected a lineage tracer. Vegetal views of stage 11 embryos are shown. E, Quantitation of the experiments shown in A-D. (F, G) *En face* view of the dorsal lip in stage 10+ embryos. Vangl2 was depleted by a unilateral injection of control or Vangl2 MO (30 ng each). F-actin staining in control (F) and Vangl2-depleted (G) blastopore cells. Arrow points to reduced apical F-actin in Vangl2-depleted cells (marked by GFP, green). Animal pole is at the top. Scale bar in F (also applies to G) is 10 μm. Dashed line indicates the midline. Arrowheads point to F-actin-enriched areas, which are reduced by Vangl2 depletion.

Fig. S3

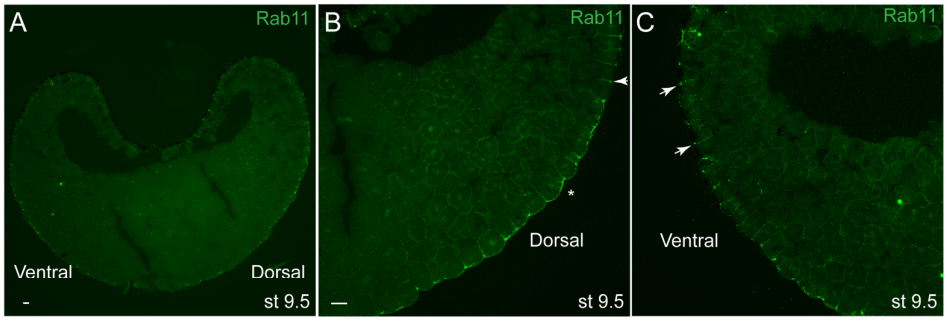

Fig. S3. Rab11 subcellular localization before gastrulation. (A-C) Cross-sections of late blastula embryos (n=10) stained for endogenous Rab11. A, Representative embryo at stage 9.5 is shown, B, Dorsal marginal zone area reveals enriched apical (asterisk) and apical junctional (arrowhead) staining. C, Rab11 is mostly at the junctions (arrowheads) in the ventral marginal zone. Scale bar is 20 μm in all panels.

Fig. S4

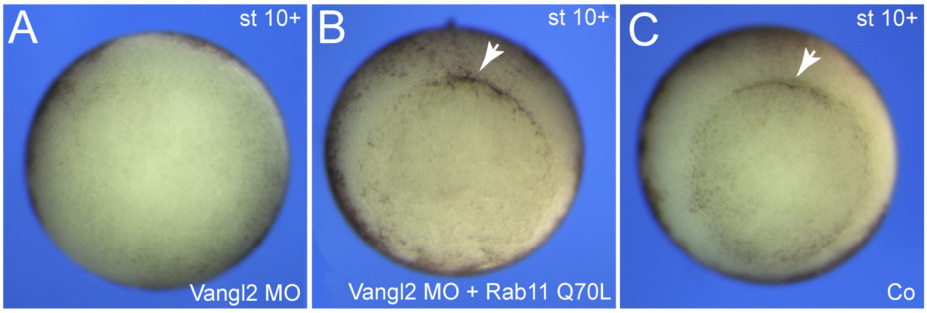

Fig. S4. Rescue of dorsal blastopore in Vangl2-depleted embryos by Rab11 RNA. (A, B) Embryos were injected with 30 ng of Vangl2 MO and 1 ng of Rab11Q70L RNA as indicated. (C) Uninjected control embryo. Vegetal views reveal the comparative morphology of the dorsal lip (arrow) for representative embryos from data in Fig. 6I.

Fig. S5

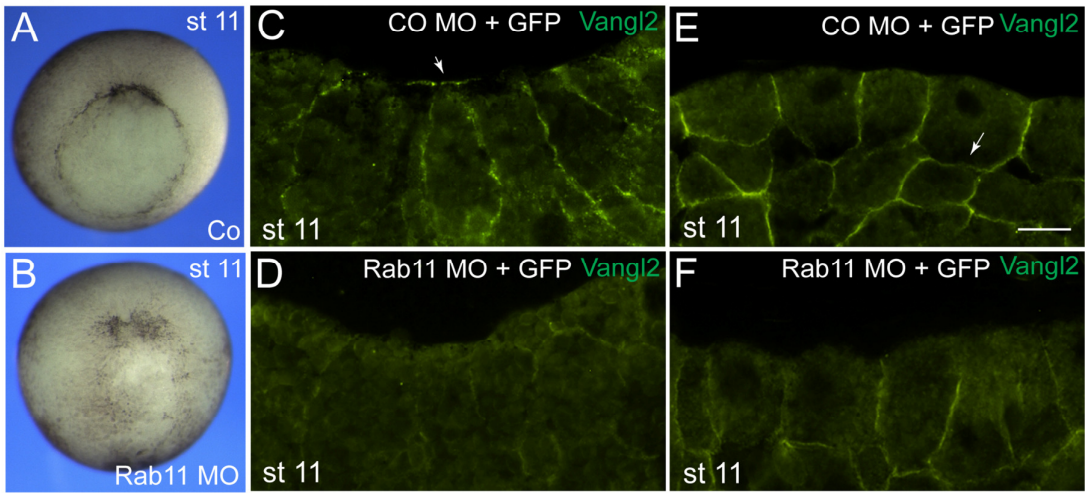

Fig. S5. Vangl2 is dissociated from the cell membrane in Rab11-depleted embryos.

Embryos were coinjected with CO MO or Vangl2 MO (30 ng each) and 100 pg of GFP RNA as lineage tracer (not shown). A, B, Morphology of control (A) and Rab11-depleted (B) embryos at st. 11, vegetal views are shown. C, D, Rab11 depletion interferes with the membrane localization of Vangl2, including the apical surface of the constricting blastopore cells (arrow). E, F, Basolateral membrane localization of Vangl2 is inhibited in ectoderm cells depleted of Rab11. Scale bar in E, also refers to C, D and F, is 20 μm.